Modeling and Optimal Regulation of Erythropoiesis Subject to Benzene Intoxication

H.T. Banks[1,2], Cammey E. Cole[1,2,4], Paul M. Schlosser[1,2,3], and Hien T. Tran[1,2]

[1] Center for Research in Scientific Computation, North Carolina State University, Raleigh, N.C.

[2] Department of Mathematics, North Carolina State University, Raleigh, N.C.

[3] CIIT Centers for Health Research, Research Triangle Park, N.C.

[4] Current address: Department of Mathematics and Computer Science, Meredith College, 3800 Hillsborough Street, Raleigh, N.C. 27607-5298, email: ColeC@meredith.edu

December 20, 2003

Abstract

Benzene (C_6H_6) is a highly flammable, colorless liquid. Ubiquitous exposures result from its presence in gasoline vapors, cigarette smoke, and industrial processes. Benzene increases the incidence of leukemia in humans when they are exposed to high doses for extended periods; however, leukemia risks in humans subjected to low exposures are uncertain. The exposure-dose-response relationship of benzene in humans is expected to be nonlinear because benzene undergoes a series of metabolic transformations, detoxifying and activating, resulting in multiple metabolites that exert toxic effects on the bone marrow.

Since benzene is a known human leukemogen, the toxicity of benzene in the bone marrow is of most importance. And because blood cells are produced in the bone marrow, we investigated the effects of benzene on hematopoiesis (blood cell production and development). An age-structured model was used to examine the process of erythropoiesis, the development of red blood cells. The existence and uniqueness of the solution of the system of coupled partial and ordinary differential equations was proven. In addition, an optimal control problem was formulated for the control of erythropoiesis. Numerical simulations were performed to compare the performance of the optimal feedback law and another feedback function that is based on the Hill function.

1 Introduction

Benzene is an ubiquitous environmental pollutant and is a component of both cigarette smoke and automobile emissions [29, 31]. It has also been a widely used solvent and a precursor for many synthetic materials [14]. Benzene is used in manufacturing products such as pesticides, drugs, detergents, lubricants, and rubber [26]. Chronic exposures to benzene result in a variety of blood and bone marrow disorders in both humans and laboratory animals [11, 16]. Increased incidence of acute myelogenous leukemia in humans resulted from high-level benzene exposures. Although the leukemogenicity of benzene has not been proven in rats or mice, benzene has been demonstrated to induce solid tumors in those species [21, 20].

Benzene exposure has long been a health concern for humans. During World War II, workers who were exposed to benzene exhibited signs of vitamin C deficiency [24]. In a nationwide investigation of benzene poisoning in China from 1972 to 1987, workers in small factories, especially in shoe manufacturing, had an incidence of aplastic anemia 5.8 times higher than the general population; the exposure levels were estimated to be between 50 and 350 ppm [28].

Much work has been done through the years on benzene dosimetry in rodents. Physiologically based pharmacokinetic (PBPK) modeling seeks to incorporate known physiological parameters such as body weight, organ volumes, and blood flow rates in particular tissues as well as known partition coefficients that have been obtained through experimentation. These models also represent uptake and metabolism by considering the chemical and physical processes that are occurring in the body. A PBPK model was developed that predicts tissue concentrations of certain metabolites in mice based on exposure using metabolic parameters obtained *in vitro* [5, 6]. Since *in vitro* metabolic parameters are also available for humans, the model could then be extrapolated to humans for risk assessment.

Since benzene is a known human leukemogen, the toxicity of benzene in the bone marrow is of most importance. Therefore, we analyzed and studied the hematopoietic cell response to benzene intoxication. Hematopoiesis is the process by which stem cells residing primarily in the bone marrow, spleen, and liver proliferate and differentiate into the major types of blood cells [2]. Erythrocytes, whose primary

function is to deliver oxygen to the tissues, are by volume the largest component of the hematopoietic system [12] and are the blood cells that are most sensitive to benzene toxicity [27]. The control of erythropoiesis is governed by the hormone erythropoietin (Epo), which is released in the bloodstream based on a negative feedback mechanism that detects partial pressures of oxygen in the blood.

Since erythrocytes are the blood cells most sensitive to benzene toxicity, in this study a modified age-structured model for the regulation of erythropoiesis that includes a death rate term for cell loss due to benzene exposure was developed [2, 3, 17, 18, 19]. We considered the response of the system after exposure by assuming initial cell depletion. This age-structured model has two major classifications of cells: precursor cells and mature cells. The precursor cells are structured by their maturity level, relative to their hemoglobin content; the mature red blood cells are structured by age. Theoretical issues as relates to the existence and uniqueness of solutions of partial differential equations were also investigated. An optimal control problem was then formulated to determine the optimal feedback mechanism by which the renal oxygen sensors detect low levels of oxygen in the blood and trigger the release of the hormone Epo. The system of coupled ordinary and partial differential equations from the aged-structured model was formulated in the weak form that provides natural means for the mathematical and numerical analysis as well as for the control formulation and synthesis. A finite element method was used to reduce the infinite dimensional system to an approximate system of ordinary differential equations for numerical studies as well as for determining the optimal feedback laws.

The organization of this article is as follows. We begin in Section 3 by examining an age-structured model for erythropoiesis, which permits incorporation of benzene toxicity into the death rate term. In Sections 4 and 5, issues of existence and uniqueness are considered for this system of coupled partial and ordinary differential equations as well as the positivity of the solutions. We write the system in the weak form in Section 6 and then consider the finite element formulation in Section 7. Several numerical studies were carried out in Section 8 to study the hematopoietic response to toxicity. We also determined an optimal form for the feedback mechanism by considering a tracking problem to regulate the normal number of red blood cells in

the body in Section 9. Section 10 includes concluding remarks and discussion of future work.

2 Physiology of Hematopoiesis

Hematopoiesis is the process by which stem cells residing primarily in the bone marrow, spleen, and liver proliferate and differentiate into the major types of blood cells, including erythrocytes, platelets, neutrophils, and macrophages [2] (see Figure 1). The blood is composed of liquid blood plasma and cellular elements suspended in

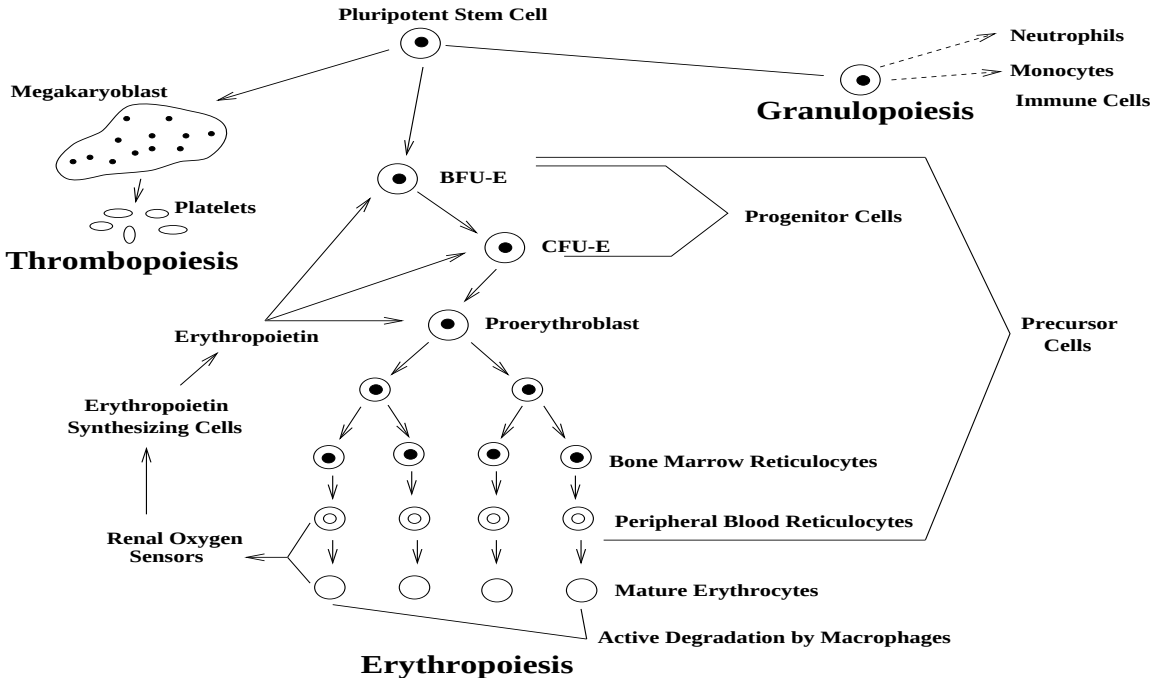

Figure 1: Schematic of cell lineage

the plasma [12]. The cellular elements make up 40% of the total blood volume and the major categories of cellular elements are erythrocytes (red blood cells), leukocytes (white blood cells), and thrombocytes (platelets) [12]. The largest (by volume) hematopoietic system produces the erythrocytes, whose primary function is to deliver oxygen to the tissues [12], and erythrocytes are believed to be the hematopoietic cells most sensitive to benzene [27]. Hemoglobin is the principal constituent of mature erythrocytes; it binds with oxygen in the lungs and releases the oxygen in the tissues [12].

Cells in the erythropoietic system can be divided into three types: stem cells, progenitor cells, and dividing and maturing cells. Stem cells have a large nuclear to cytoplasmic ratio and under normal conditions are not in the cell cycle [23]. Progenitor cells comprise 1% of the total hemopoietic population and are the transit population of stem cells [23]. They expend their energy in production of maturing progeny and have little to no capacity to self-generate. The two major classes of progenitor cells in the erythroid lineage include Erythroid Burst-Forming Units (BFU-Es) and Erythroid Colony-Forming Units (CFU-Es). BFU-Es are a self-sustaining population that show minimal signs of differentiation but respond to the appropriate hormone to accelerate proliferation in response to physiological needs [23]. CFU-Es form small colonies that are the equivalent of one of the subclones of a multicentric colony formed by BFU-Es and they are not self-sustaining [23]. Dividing and maturing cells are the majority of cells present in hemopoietic tissues [23]. The least mature of these cells have considerable proliferation capacity but this capacity is not strictly fixed; it is dependent on the level of stimulation exerted by relevant growth factors [23]. These cells eventually mature to a postmitotic stage, after which no further cell division is possible [23]. We note that the cells in each succeeding compartment (stem, progenitor, dividing/maturing) are more numerous than in the proceeding compartment [23].

Within erythrocyte maturation, the most immature cell belonging to the erythrocyte series is the proerythroblast [10]. The stages of cells can be distinguished by increasing levels of hemoglobin [2]. Once cells become reticulocytes they stop dividing and mature by increasing their hemoglobin content [2]. Reticulocytes lose their nuclei and become mature erythrocytes [2].

The control of erythropoiesis is governed by the hormone erythropoietin (Epo), which is an acidic glycoprotein as well as a poor antigen, that stimulates red blood cell production [9]. It is produced primarily in the kidneys, with 90% of Epo being secreted by renal tubular epithelial cells when blood is unable to deliver oxygen [12]. Thus, Epo acts by controlling the rate of differentiation of bone marrow cells and is released in the bloodstream based on a negative feedback mechanism that detects partial pressures of oxygen in the blood. It has a relatively short half-life, creating a rapid response to the changing conditions in the body [2, 30].

The appropriate form of the function that might represent this feedback of Epo is unknown. Previously, a Hill function has been used; this function is often used to represent enzyme kinetics but it has no physiological basis. We use control theory to formulate a tracking problem in which we seek an optimal form of the feedback which causes the release of Epo such that the body produces the cells necessary to maintain the normal level of red blood cells in the body.

3 Model Development

With its many stages of development, and because cells in differing stages have different properties, erythropoiesis lends itself naturally to age-structured modeling [2, 3, 17, 18, 19]. Since it is known that erythrocytes are the blood cells most sensitive to benzene toxicity, in this study a modified age-structured model for the regulation of erythropoiesis that included a death rate term for cell loss due to benzene exposure was developed. More specifically, the concentrations of phenol and hydroquinone, which are two of benzene metabolites, in the richly perfused tissues (which includes the bone marrow) found from the PBPK model could be used as time-course inputs to the age-structured model through precursor cell death rate term [5, 6]. At this point though, we assumed a constant death rate from benzene toxicity.

The following model is based on work by Jacques Bélair, Michael Mackey, and Joseph Mahaffy [2, 3, 17, 18, 19]. A list of abbreviations and symbols used in the model can be found in the Appendix. This age-structured model has two major classifications of cells: precursor cells $p(t, \mu)$ and mature cells $m(t, \nu)$. The precursor cells include progenitor cells, dividing cells, and reticulocytes; the mature cells are the erythrocytes in the circulating blood. The precursor cells are structured by their maturity level μ, relative to their hemoglobin content; the mature red blood cells are structured by age ν. The concentration of the hormone Epo is given by $E(t)$. We denote the velocity of maturation of precursor cells by $V(E)$, while the rate of aging of mature cells is given by W. The birth rate of precursor cells is given by $\beta(\mu)$ and $\alpha(t)$ is the death rate; the death rate of mature cells is given by $\gamma(\nu)$. The number of cells recruited into the proliferating precursor population is proportional to the concentration of Epo; S_0 is the constant of proportionality. A basic schematic of the

model is given in Figure 2, which is similar to the one used in Bélair et al. [2].

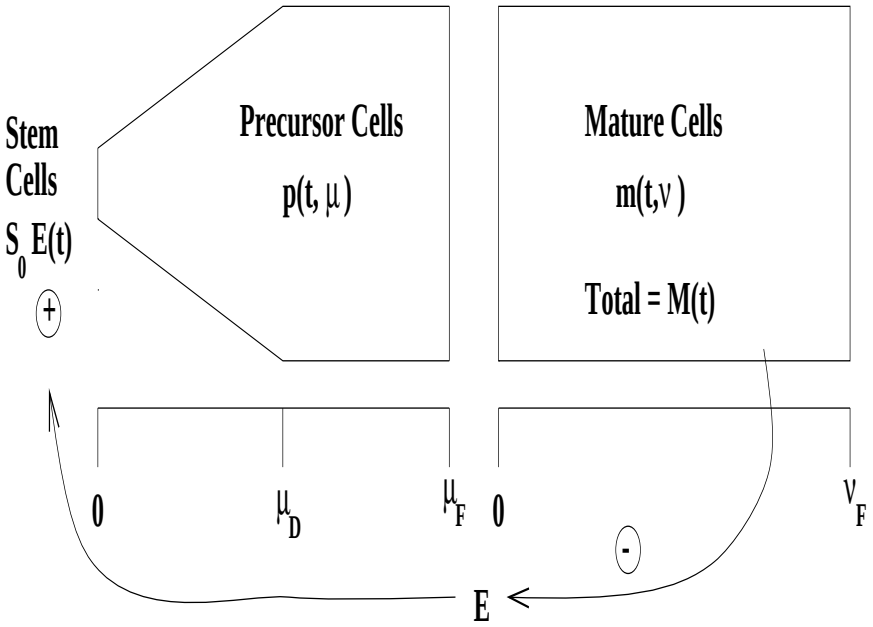

Figure 2: Schematic of erythropoiesis model

We begin by deriving the equation for the precursor cells. First we make the following assumptions:

1. The maturity of any individual cell is dynamically described by

$$\frac{d\mu}{dt} = V(E(t)).$$

We make a further simplification and assume that for this model $V(E(t)) = 1$. Thus,

$$\frac{d\mu}{dt} = 1$$

which means

$$\mu = t + t_0.$$

For our particular case, this means $\mu = t$ but in general this is not the case. If $V(E(t))$ was not equal to 1, μ would be given by some function of $E(t)$.

2. All maturity levels of precursor cells have the same death rate

$$\alpha(t) = \alpha_0 + k_C C_R^{PH}(t) C_R^{HQ}(t),$$

where $C_R^{PH}(t)$ and $C_R^{HQ}(t)$ are the concentrations of phenol and hydroquinone respectively in the richly perfused tissues containing the bone marrow, which

are obtained from the PBPK model described in [5] and [6]. Here we make the simplifying assumption that α is constant.

3. The birth rate is dependent upon maturity level

$$\beta(\mu) \quad = \quad \begin{cases} \beta & \mu < \mu_D \\ 0 & \mu \geq \mu_D \end{cases},$$

where β is a nonnegative constant and μ_D is the point at which all cell division stops but the cell continues to mature.

4. There is a level of least maturity and a level of greatest maturity $(0 = \mu_0 \leq \mu \leq \mu_F)$.

5. The number of precursor cells at the smallest maturity level is equal to the number of stem cells being recruited into the precursor cell population, which is proportional to the concentration of Epo in the system. Thus,

$$p(t, 0) \quad = \quad S_0 \, E(t).$$

6. The number of precursor cells at the greatest maturity level is equal to the number of mature cells at the smallest age level:

$$p(t, \mu_F) = m(t, 0).$$

Let $P^T(t)$ be the total population of precursor cells at time t. We will use the following notation to represent the population of precursor cells from maturity level a to b at time t_1:

$$P^T_{a,b}(t_1) = \int_a^b p(t_1, \psi) d\psi.$$

Under the previously stated assumptions, let us now derive the equation which represents the precursor cells by examining the flux balance. This is given by:

rate of change in population in the maturity interval (a, b)

= rate of cells entering the interval - rate of cells leaving the interval

+ birth rate term - death rate term.

Letting the interval be $[\mu, \mu + \Delta\mu]$, and using flux balance, we obtain

$$\frac{\partial}{\partial t} \int_\mu^{\mu+\Delta\mu} p(t, \xi) d\xi$$

$$= 1 \times p(t, \mu) - 1 \times p(t, \mu + \Delta\mu) + \int_\mu^{\mu+\Delta\mu} \beta(\xi) p(t, \xi) d\xi - \int_\mu^{\mu+\Delta\mu} \alpha p(t, \xi) d\xi$$

where the maturity rate is assumed to be 1. Divide by $\Delta\mu$ and take the limit as $\Delta\mu$ approaches 0. We find

$$\frac{\partial}{\partial t}p(t,\mu) = -\frac{\partial}{\partial \mu}p(t,\mu) + [\beta(\mu) - \alpha]p(t,\mu). \quad (1)$$

From assumptions previously given, we have the boundary condition given by

$$p(t,0) = S_0\, E(t). \quad (2)$$

In a similar manner to that for the precursor cell equation and under similar assumptions with the exception that birth only occurs at the smallest age and is equal to the number of precursor cells that have reached full maturity μ_F, we find that the population of mature cells is represented by:

$$\frac{\partial m(t,\nu)}{\partial t} + \frac{\partial m(t,\nu)}{\partial \nu} = -\gamma m(t,\nu), \quad 0 < \nu \leq \nu_F \quad (3)$$

$$m(t,0) = p(t,\mu_F). \quad (4)$$

We note that $\mu_F < \nu_F$.

Finally, the equation for Epo depends on the following biological properties:

rate of change of concentration of Epo in system

$$= -\text{ decay rate of Epo} \times \text{concentration of Epo}$$
$$+ \text{ feedback of Epo released from kidneys.}$$

Here, we represent Epo by the following equation:

$$\frac{dE}{dt} = -k_E E + f(m)(t), \quad (5)$$

where k_E is the decay rate of Epo and $f(m)(t)$ is the feedback function, which is usually assumed in the form of a Hill function in the current literature:

$$f(m)(t) = \frac{a}{1 + K\,[M(t)]^r}, \quad (6)$$

where $a, K > 0$ and

$$M(t) = \int_0^{\nu_F} m(t,\nu)d\nu \quad (7)$$

is the total number of mature cells. The Hill function is often used to accurately approximate rates in enzyme kinetic problems but it has no physiological basis in this particular context [2].

Thus, the model is represented by the following system of equations:

$$\begin{aligned}
\frac{\partial p(t,\mu)}{\partial t} + \frac{\partial p(t,\mu)}{\partial \mu} &= [\beta(\mu) - \alpha]p(t,\mu), \quad 0 < \mu \leq \mu_F && (8)\\
\frac{\partial m(t,\nu)}{\partial t} + \frac{\partial m(t,\nu)}{\partial \nu} &= -\gamma m(t,\nu), \quad 0 < \nu \leq \nu_F && (9)\\
\frac{dE}{dt} + k_E E &= f(m)(t) && (10)\\
p(t,0) &= S_0\, E(t) && (11)\\
p(t,\mu_F) &= m(t,0) && (12)\\
p(0,\mu) &= p_0(\mu) && (13)\\
m(0,\nu) &= m_0(\nu) && (14)\\
E(0) &= E_0, && (15)
\end{aligned}$$

where $p_0(\mu)$ and $m_0(\nu)$ are nonnegative continuous functions for all μ and ν respectively, and α, γ, k_E, S_0, and E_0 are nonnegative constants. We will show in Section 5 that $m_0(\nu)$ being a nonnegative function will guarantee that $M(t)$ is nonnegative, thereby alleviating the possibility of a singularity in $f(m)(t)$.

4 Existence and Uniqueness

In this section, we establish the existence and uniqueness of solutions to our matematical model given by equations (8) - (15).

Since equations (8) and (9) are linear, first-order hyperbolic partial differential equations, we will use the method of characteristics to find a solution for each of the partial differential equations and then use these to rewrite the nonlinear term in the ordinary differential equation.

Consider the equation

$$\begin{aligned}
p_t(t,\mu) + p_\mu(t,\mu) &= [\beta(\mu) - \alpha]p(t,\mu) && (16)\\
p(0,\mu) &= p_0(\mu)\\
p(t,0) &= S_0 E(t).
\end{aligned}$$

Let $P(s) = p(t(s), \mu(s))$, where s is a parameterization in $t - \mu$ space. Then

$$\begin{aligned}
\frac{dP(s)}{ds} &= \frac{d}{ds} p(t(s), \mu(s))\\
&= \frac{\partial p}{\partial t}\frac{dt}{ds} + \frac{\partial p}{\partial \mu}\frac{d\mu}{ds}. && (17)
\end{aligned}$$

If

$$\frac{dt}{ds} = 1 \tag{18}$$

$$\frac{d\mu}{ds} = 1, \tag{19}$$

then equation (16) can be rewritten as

$$\frac{dP(s)}{ds} = [\beta(\mu(s)) - \alpha]P(s),$$

which can be solved using separation of variables to find the solution

$$P(s) = P(0)e^{\int_0^s [\beta(\mu(\psi)) - \alpha]d\psi}. \tag{20}$$

The solution to equations (18) and (19), given by

$$t(s) = s + t(0)$$

$$\mu(s) = s + \mu(0),$$

defines the characteristic lines along which the solution given by equation (20) is valid. Figure 3 depicts these characteristics, where the regions of solution $p(t, \mu)$ are divided by the curve $t = \mu$ which passes through $(0, 0)$.

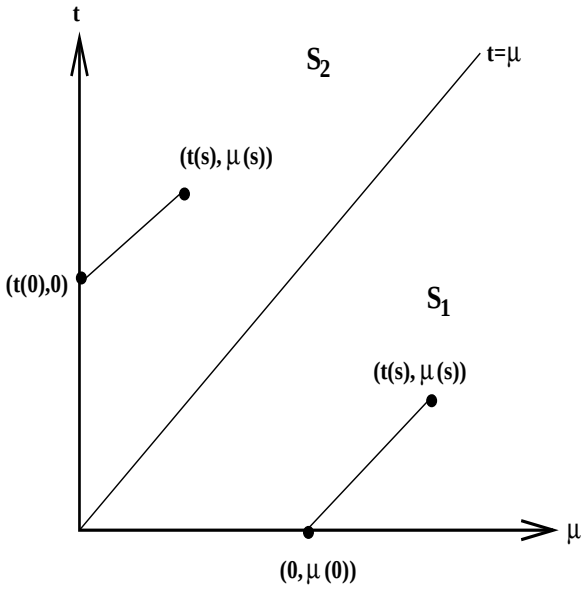

Figure 3: Regions of solution of $p(t, \mu)$

In region S_1, where $t \leq \mu$, our solution is determined by our initial condition, $(0, \mu(0))$. Thus we have

$$\begin{aligned} t(s) &= s \\ \mu(s) &= s + \mu(0), \end{aligned}$$

which gives us

$$\mu(s) = \mu(0) + t(s).$$

Now, using our initial condition in equation (20), we find

$$\begin{aligned} P(0) &= p(t(0), \mu(0)) \\ &= p(0, \mu - t) \\ &= p_0(\mu - t). \end{aligned}$$

Therefore, for (t, μ) in S_1,

$$p(t, \mu) = p_0(\mu - t) e^{\int_0^t [\beta(\mu(s)) - \alpha] ds}.$$

For $(t(s), \mu(s)) \in S_2$, where $t > \mu$, the solution is dominated by the boundary condition. Here,

$$\begin{aligned} t(s) &= s + t(0) \\ \mu(s) &= s. \end{aligned}$$

Thus,

$$t(0) = t - \mu.$$

In addition, for $(t(s), \mu(s)) \in S_2$, we have

$$\begin{aligned} P(0) &= p(t(0), \mu(0)) \\ &= p(t - \mu, 0). \end{aligned}$$

Therefore, our solution for (t, μ) in S_2 is given by

$$p(t, \mu) = S_0 E(t - \mu) e^{\int_0^\mu [\beta(s) - \alpha] ds}.$$

Thus, the solution of equation (16) is given by

$$p(t, \mu) = \begin{cases} p_0(\mu - t) e^{\int_0^t [\beta(\mu(s)) - \alpha] ds} & t \leq \mu \\ S_0 E(t - \mu) e^{\int_0^\mu [\beta(s) - \alpha] ds} & t > \mu. \end{cases} \tag{21}$$

In a like manner, we find that the solution of

$$\begin{aligned} m_t(t,\nu) + m_\nu(t,\nu) &= -\gamma m(t,\nu) \\ m(0,\nu) &= m_0(\nu) \\ m(t,0) &= p(t,\mu_F) \end{aligned}$$

is given by

$$m(t,\nu) = \begin{cases} m_0(\nu - t)e^{-\gamma t} & t \leq \nu \\ p(t-\nu,\mu_F)e^{-\gamma\nu} & t > \nu. \end{cases} \tag{22}$$

Figure 4 summarizes the dependence of the solution of $m(\cdot,\cdot)$ on the initial and boundary condition and on the function $E(\cdot)$. This figure suggests that, for establishing existence and uniqueness to the mathematical model given by equations (8) - (15), we need to split the time domain into four intervals: $[0,\mu_F]$, $[\mu_F,\nu_F]$, $[\nu_F,\nu_F+\mu_F]$, and $[\nu_F+\mu_F,t_F]$ where $t_F > \nu_F + \mu_F$.

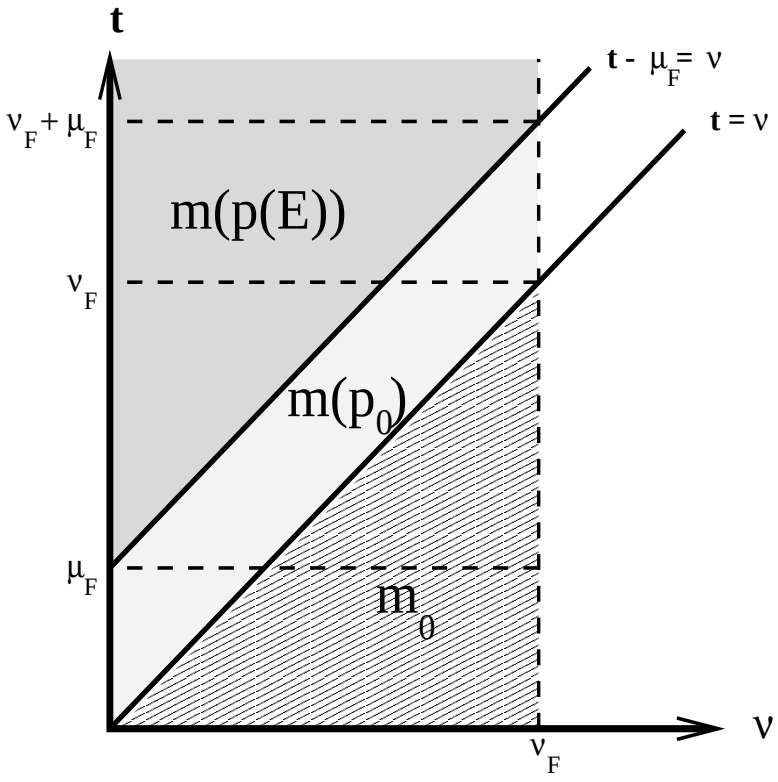

Figure 4: Regions of solution of $m(t,\nu)$

From the expression for $M(t)$ we have, for $0 \leq t \leq \mu_F$,

$$M(t) = \int_0^{\nu_F} m(t,\nu)d\nu$$

$$
\begin{aligned}
&= \int_0^t m(t,\nu)d\nu + \int_t^{\nu_F} m(t,\nu)d\nu \\
&= \int_0^t p(t-\nu,\mu_F)e^{-\gamma\nu}d\nu + \int_t^{\nu_F} m_0(\nu-t)e^{-\gamma t}d\nu. \qquad (23)
\end{aligned}
$$

Dividing the integral in this manner is motivated by Figure 4. Now consider the integral

$$\int_0^t p(t-\nu,\mu_F)e^{-\gamma\nu}d\nu,$$

which, for $0 \le t \le \mu_F$, is given in terms of $p_0(\cdot)$ as

$$\int_0^t p(t-\nu,\mu_F)e^{-\gamma\nu}d\nu = \int_0^t p_0(\mu_F - t + \nu)e^{\int_0^{t-\nu}[\beta(\mu(s))-\alpha]ds}e^{-\gamma\nu}d\nu.$$

Therefore,

$$M(t) = \int_0^t p_0(\mu_F - t + \nu)e^{\int_0^{t-\nu}[\beta(\mu(s))-\alpha]ds}e^{-\gamma\nu}d\nu + \int_t^{\nu_F} m_0(\nu-t)e^{-\gamma t}d\nu \qquad (24)$$

for $0 \le t \le \mu_F$. Thus, $f(m)(t)$ depends only on known parameters and given initial functions $p_0(\cdot)$ and $m_0(\cdot)$. That is, $f(m)(t)$ depends explicitly on t and will be denoted by $f(t)$ for $t \in [0, \mu_F]$. This will hold for $f(m)$ assumed in the form of a Hill function as in equation (6) or for any other form of f as long as the dependence of f on m is only through the total number M of mature cells as given in equation (7).

Therefore, the equation for $E(t)$ depends only on the known initial conditions of the partial differential equations. Note that the differential equation for $E(t)$ is now linear with a continuous forcing term

$$\frac{d}{dt}E(t) = -k_E E(t) + f(t). \qquad (25)$$

Therefore, the solution $E(t)$, $0 \le t \le \mu_F$, exists and is unique since $f(t)$ is a continuous function [4]. Thus, by the method of characteristics, we have a unique solution for $p(t,\mu)$ and $m(t,\nu)$ for $t \in [0, \mu_F]$.

Now consider $\mu_F < t \le 2\mu_F$, where we assume $2\mu_F \le \nu_F$. Here,

$$
\begin{aligned}
M(t) &= \int_0^{\nu_F} m(t,\nu)d\nu \\
&= \int_0^{t-\mu_F} m(t,\nu)d\nu + \int_{t-\mu_F}^t m(t,\nu)d\nu + \int_t^{\nu_F} m(t,\nu)d\nu \\
&= \int_0^{t-\mu_F} p(t-\nu,\mu_F)e^{-\gamma\nu}d\nu + \int_{t-\mu_F}^t p(t-\nu,\mu_F)e^{-\gamma\nu}d\nu \\
&\quad + \int_t^{\nu_F} m_0(\nu-t)e^{-\gamma t}d\nu
\end{aligned}
$$

$$
\begin{aligned}
&= \int_0^{t-\mu_F} S_0 E(t-\nu-\mu_F) e^{\beta\mu_D-\alpha\mu_F-\gamma\nu} d\nu \\
&\quad + \int_{t-\mu_F}^{t} p_0(\mu_F-t+\nu) e^{\int_0^{t-\nu}[\beta(\mu(s))-\alpha]ds} e^{-\gamma\nu} d\nu \\
&\quad + \int_t^{\nu_F} m_0(\nu-t) e^{-\gamma t} d\nu \\
&= S_0 e^{\beta\mu_D-\alpha\mu_F-\gamma(t-\mu_F)} \int_0^{t-\mu_F} E(w) e^{\gamma w} dw \\
&\quad + \int_{t-\mu_F}^{t} p_0(\mu_F-t+\nu) e^{\int_0^{t-\nu}[\beta(\mu(s))-\alpha]ds} e^{-\gamma\nu} d\nu \\
&\quad + \int_t^{\nu_F} m_0(\nu-t) e^{-\gamma t} d\nu. \qquad (26)
\end{aligned}
$$

Since $p_0(\cdot)$ and $m_0(\cdot)$ are known, let

$$
h(t) = \int_{t-\mu_F}^{t} p_0(\mu_F-t+\nu) e^{\int_0^{t-\nu}[\beta(\mu(s))-\alpha]ds} e^{-\gamma\nu} d\nu + \int_t^{\nu_F} m_0(\nu-t) e^{-\gamma t} d\nu.
$$

Thus, we can write

$$
M(t) = S_0 e^{\beta\mu_D-\alpha\mu_F-\gamma(t-\mu_F)} \int_0^{t-\mu_F} E(w) e^{\gamma w} dw + h(t).
$$

We now differentiate $M(t)$, obtaining

$$
\begin{aligned}
\frac{d}{dt}M(t) &= -\gamma S_0 e^{\beta\mu_D-\alpha\mu_F-\gamma(t-\mu_F)} \int_0^{t-\mu_F} E(w) e^{\gamma w} dw \\
&\qquad + S_0 e^{\beta\mu_D-\alpha\mu_F-\gamma(t-\mu_F)} E(t-\mu_F) e^{\gamma(t-\mu_F)} + h'(t) \\
&= -\gamma S_0 e^{\beta\mu_D-\alpha\mu_F-\gamma(t-\mu_F)} \int_0^{t-\mu_F} E(w) e^{\gamma w} dw \\
&\qquad + S_0 e^{\beta\mu_D-\alpha\mu_F} E(t-\mu_F) + h'(t) \\
&= -\gamma \left[M(t) - h(t)\right] + S_0 e^{\beta\mu_D-\alpha\mu_F} E(t-\mu_F) + h'(t) \\
&= -\gamma M(t) + S_0 e^{\beta\mu_D-\alpha\mu_F} E(t-\mu_F) + \hat{h}(t), \qquad (27)
\end{aligned}
$$

where $\hat{h}(t) = \gamma h(t) + h'(t)$. Thus, for $t \in [\mu_F, 2\mu_F]$, where $2\mu_F \leq \nu_F$, the method of characteristics replaces the age-structured population equations for p and m (coupled with that for E) by a a coupled delay differential system for the total number of mature cells, $M(t)$, and the concentration of Epo, $E(t)$. The new system of delay differential equations is given by:

$$
\begin{aligned}
\frac{d}{dt}M(t) &= -\gamma M(t) + S_0 e^{\beta\mu_D-\alpha\mu_F} E(t-\mu_F) + \hat{h}(t) \qquad (28) \\
\frac{d}{dt}E(t) &= -k_E E(t) + \frac{a}{1+K[M(t)]^r} \qquad (29)
\end{aligned}
$$

for $t \in [\mu_F, 2\mu_F]$ with $2\mu_F \leq \nu_F$ and initial conditions

$$M(\mu_F) = \int_0^{\nu_F} m(\mu_F, \nu) d\nu,$$

where $m(\mu_F, \nu)$ is given by equation (22) and $E(t)$ is the solution of equation (25) for $t \in [0, \mu_F]$. Thus, we have an equation of the form

$$\dot{\vec{x}}(t) = \vec{g}(t, \vec{x}(t), \vec{x}(t - \mu_F)), \tag{30}$$

where

$$\vec{x}(t) = \begin{bmatrix} M(t) \\ E(t) \end{bmatrix} \tag{31}$$

$$\vec{g}(t, \vec{\xi}_{(1)}, \vec{\xi}_{(2)}) = \begin{bmatrix} -\gamma \xi_{(1)1} + S_0 e^{\beta\mu_D - \alpha\mu_F} \xi_{(2)2} + \hat{h}(t) \\ -k_E \xi_{(1)2} + \frac{a}{1 + K\xi_{(1)1}^r} \end{bmatrix}. \tag{32}$$

Certainly, $\vec{g}$ is continuous, and so are the partial derivatives:

$$\begin{aligned}
\frac{\partial g_1}{\partial \xi_{(1)1}} &= -\gamma \\
\frac{\partial g_1}{\partial \xi_{(1)2}} &= 0 \\
\frac{\partial g_1}{\partial \xi_{(2)1}} &= 0 \\
\frac{\partial g_1}{\partial \xi_{(2)2}} &= S_0 e^{\beta\mu_D - \alpha\mu_F} \\
\frac{\partial g_2}{\partial \xi_{(1)1}} &= -\frac{aKr\xi_{(1)1}^{r-1}}{[1 + K\xi_{(1)1}^r]^2} \\
\frac{\partial g_2}{\partial \xi_{(1)2}} &= -k_E. \\
\frac{\partial g_2}{\partial \xi_{(2)1}} &= 0 \\
\frac{\partial g_2}{\partial \xi_{(2)2}} &= 0.
\end{aligned}$$

In addition, the partial derivatives are globally bounded; thus, $\vec{g}$ is globally Lipschitz with respect to $\xi_{(1)}$. On the interval $[\mu_F, 2\mu_F]$ equation (30) becomes

$$\dot{\vec{x}}(t) = \vec{g}(t, \vec{x}(t), \vec{x}(t - \mu_F)) \equiv \vec{h}(t, \vec{x}(t)) \tag{33}$$

since $E(t)$ for $t \in [0, \mu_F]$ is a known function. Further, $\vec{h}(t, \vec{x})$ is continuous in both arguments and Lipschitz in $\vec{x}$. By a standard existence result for ordinary differential

equations [25], the solution of $\dot{\vec{x}} = \vec{h}(t, \vec{x})$ exists on $[\mu_F, 2\mu_F]$ and is unique. This gives us an initial function for the solution on the interval $[2\mu_F, 3\mu_F]$; simple induction arguments yield existence and uniqueness on $[\mu_F, \nu_F]$. This is known as the method of steps [7, 8, 22], which is a standard method for establishing existence and uniqueness of solutions to delay differential equations.

Once $t > \nu_F$, we can not write $M(t)$ in the same manner. For $t \in [\nu_F, \nu_F + \mu_F]$,

$$\begin{aligned}
M(t) &= \int_0^{\nu_F} m(t,\nu)d\nu \\
&= \int_0^{t-\mu_F} m(t,\nu)d\nu + \int_{t-\mu_F}^{\nu_F} m(t,\nu)d\nu \\
&= \int_0^{t-\mu_F} p(t-\nu,\mu_F)e^{-\gamma\nu}d\nu + \int_{t-\mu_F}^{\nu_F} p(t-\nu,\mu_F)e^{-\gamma\nu}d\nu \\
&= \int_0^{t-\mu_F} S_0 E(t-\nu-\mu_F)e^{\beta\mu_D-\alpha\mu_F-\gamma\nu}d\nu \\
&\qquad + \int_{t-\mu_F}^{\nu_F} p_0(\mu_F-t+\nu)e^{\int_0^{t-\nu}[\beta(\mu(s))-\alpha]ds}e^{-\gamma\nu}d\nu \\
&= S_0 e^{\beta\mu_D-\alpha\mu_F-\gamma(t-\mu_F)} \int_0^{t-\mu_F} E(w)e^{\gamma w}dw \\
&\qquad + \int_{t-\mu_F}^{\nu_F} p_0(\mu_F-t+\nu)e^{\int_0^{t-\nu}[\beta(\mu(s))-\alpha]ds}e^{-\gamma\nu}d\nu. \qquad (34)
\end{aligned}$$

Following techniques similar to those above, we can write a new system of delay differential equations for $t \in [\nu_F, \nu_F + \mu_F]$:

$$\frac{d}{dt}M(t) = -\gamma M(t) + S_0 e^{\beta\mu_D-\alpha\mu_F}E(t-\mu_F) + \tilde{h}(t) \qquad (35)$$

$$\frac{d}{dt}E(t) = -k_E E(t) + \frac{a}{1+K[M(t)]^r} \qquad (36)$$

for $t \in [\nu_F, \nu_F + \mu_F]$ where

$$\begin{aligned}
\tilde{h}(t) = \frac{d}{dt}&\left[\int_{t-\mu_F}^{t} p_0(\mu_F-t+\nu)e^{\int_0^{t-\nu}[\beta(\mu(s))-\alpha]ds}e^{-\gamma\nu}d\nu\right] \\
&+\gamma\int_{t-\mu_F}^{t} p_0(\mu_F-t+\nu)e^{\int_0^{t-\nu}[\beta(\mu(s))-\alpha]ds}e^{-\gamma\nu}d\nu
\end{aligned}$$

with initial conditions

$$M(\nu_F) = \int_0^{\nu_F} m(\nu_F,\nu)d\nu,$$

where $m(\nu_F, \nu)$ is given by equation (22) and $E(t)$ is the solutions of systems previously solved for $t \in [0, \nu_F]$. As shown previously using the method of steps and theory for ordinary differential equations, we can establish that the solution exists and is unique for $t \in [\nu_F, \nu_F + \mu_F]$.

Next we consider the case when $t > \nu_F + \mu_F$:

$$\begin{aligned} M(t) &= \int_0^{\nu_F} m(t,\nu)d\nu \\ &= \int_0^{\nu_F} p(t-\nu,\mu_F)e^{-\gamma\nu}d\nu \\ &= \int_0^{\nu_F} S_0 E(t-\nu-\mu_F)e^{\beta\mu_D-\alpha\mu_F}e^{-\gamma\nu}d\nu \\ &= S_0 e^{\beta\mu_D-\alpha\mu_F-\gamma(t-\mu_F)}\int_{t-\nu_F-\mu_F}^{t-\mu_F} E(w)e^{\gamma w}dw. \end{aligned} \tag{37}$$

Differentiating equation (37), using Leibniz's Rule to differentiate the integral on the right-hand side, we obtain

$$\begin{aligned} \frac{d}{dt}M(t) &= -\gamma S_0 e^{\beta\mu_D-\alpha\mu_F-\gamma(t-\mu_F)}\int_{t-\nu_F-\mu_F}^{t-\mu_F} E(w)e^{\gamma w}dw \\ &\quad + S_0 e^{\beta\mu_D-\alpha\mu_F-\gamma(t-\mu_F)}\Big[E(t-\mu_F)e^{\gamma(t-\mu_F)} - E(t-\nu_F-\mu_F)e^{\gamma(t-\nu_F-\mu_F)}\Big] \\ &= -\gamma M(t) + S_0 e^{\beta\mu_D-\alpha\mu_F}\Big[E(t-\mu_F) - E(t-\nu_F-\mu_F)e^{-\gamma\nu_F}\Big]. \end{aligned} \tag{38}$$

Thus for large time behavior with $t > \nu_F + \mu_F$, the method of characteristics again replaces the age-structured population equations for p and m along with E by a delay differential equation system for the total number of mature cells, $M(t)$, and the concentration of Epo, $E(t)$. The new system of delay differential equations is given by:

$$\frac{d}{dt}M(t) = -\gamma M(t) + S_0 e^{\beta\mu_D-\alpha\mu_F}[E(t-\mu_F) - E(t-\nu_F-\mu_F)e^{-\gamma\nu_F}] \tag{39}$$

$$\frac{d}{dt}E(t) = -k_E E(t) + \frac{a}{1+K[M(t)]^r}, \tag{40}$$

for $t > \nu_F + \mu_F$ with initial conditions

$$M(\nu_F+\mu_F) = \int_0^{\nu_F} m(\nu_F+\mu_F,\nu)d\nu.$$

Here $m(\nu_F+\mu_F,\nu)$ is given by equation (22) and the initial values of $E(t)$ are the solutions of systems previously solved for $t \in [0, \nu_F+\mu_F]$. Using arguments similar to those above, we find by the method of steps and a standard existence result for ordinary differential equations [25] that the solution exists and is unique on $[\nu_F+\mu_F, 2(\nu_F+\mu_F)]$. This gives us an initial function for the solution on the interval $[2(\nu_F+\mu_F), 3(\nu_F+\mu_F)]$; simple induction arguments yield existence and uniqueness on $[\nu_F+\mu_F, t_F]$ for any $t_F > \nu_F+\mu_F$ [7, 8, 22].

Therefore, since $E(t)$ exists and is unique for $t \in [0, t_F]$ for all $t_F > 0$, $p(t, \mu)$ and $m(t, \nu)$ exist and are unique for all $t_F > 0$, all $\mu \in [0, \mu_F]$, and all $\nu \in [0, \nu_F]$ by the method of characteristics.

5 Positivity of Solutions

Since p and m represent the number of cells and E is the concentration of a hormone, none of which can be negative physically, we need to show that our system has a nonnegative solution when the initial conditions are nonnegative.

We begin by assuming the following:

$$E(0) = E_0 \geq 0 \tag{41}$$

$$p(0, \mu) = p_0(\mu) \geq 0 \text{ for all } \mu \in (0, \mu_F] \tag{42}$$

$$m(0, \nu) = m_0(\nu) \geq 0 \text{ for all } \nu \in (0, \nu_F]. \tag{43}$$

Then $M(t)$ given in equation (24) is nonnegative since p_0 and m_0 are nonnegative; thus, $f(t)$ in equation (25) is nonnegative, which gives us a nonnegative function $E(t)$ for $t \in [0, \mu_F]$. It follows that $p(t, \mu)$ and $m(t, \nu)$ are nonnegative for $t \in [0, \mu_F]$ and for all $\mu \in [0, \mu_F]$ and $\nu \in [0, \nu_F]$.

For each of the systems of delay differential equations, the right-hand side of these equations is nonnegative since equations $M(t)$ and $E(t)$ are nonnegative on the previous time intervals. Therefore, $E(t)$ is nonnegative for $t \in [0, t_F)$ for all $t_F > 0$.

Hence, since $p_0(\mu)$ is nonnegative for all μ and $E(t)$ is nonnegative for all t, $p(t, \mu)$ is nonnegative for all t and all μ. Since $m_0(\nu)$ is nonnegative for all ν and $p(t, \mu_F)$ is nonnegative for all t, $m(t, \nu)$ is nonnegative for all t and all ν.

Therefore, if we assume all initial conditions are nonnegative, the solution of the system given by equations (8) - (15) has nonnegative components.

6 Weak Formulation

In this section, we restate system given by equations (8) - (15) in terms of a weak or variational formulation. The weak formulation provides a natural setting for the

numerical approximation to the solution of equations (8) - (15) by the finite element method and for the control design and synthesis.

6.1 Preliminaries

Define the domains for the maturity levels (ML) and age levels (AL) respectively:

$$\begin{aligned} \Omega_{ML} &= \{\mu : 0 < \mu \leq \mu_F\} \\ \Omega_{AL} &= \{\nu : 0 < \nu \leq \nu_F\}. \end{aligned}$$

We also use the following notational conventions:

$$\begin{aligned} H^1_{ML} &= H^1(\Omega_{ML}) \\ H^1_{AL} &= H^1(\Omega_{AL}) \\ L^2_{ML} &= L^2(\Omega_{ML}) \\ L^2_{AL} &= L^2(\Omega_{AL}). \end{aligned}$$

and define the state space

$$\mathcal{V} = H^1_{ML} \times H^1_{AL} \times \Re.$$

We define the inner product

$$\langle \phi, \psi \rangle_{L^2_{ML}} = \int_0^{\mu_F} \phi(\mu)\psi(\mu)d\mu$$

for $\phi, \psi \in L^2_{ML}$ and the inner product

$$\langle \phi, \psi \rangle_{L^2_{AL}} = \int_0^{\nu_F} \phi(\nu)\psi(\nu)d\nu$$

for $\phi, \psi \in L^2_{AL}$.

6.2 Problem Formulation

We begin by considering the partial differential equation for $p(t, \mu)$. We multiply equation (8) by a test function $\phi \in H^1_{ML}$, followed by integration by parts. Thus, we have

$$\langle \dot{p}, \phi \rangle_{L^2_{ML}} - \langle p, \phi' \rangle_{L^2_{ML}} + p(\mu_F)\phi(\mu_F) - p(0)\phi(0) = \langle [\beta(\mu) - \alpha]\, p, \phi \rangle_{L^2_{ML}}.$$

Upon substituting the natural boundary condition from equation (11), we obtain

$$\langle \dot{p}, \phi \rangle_{L^2_{ML}} - \langle p, \phi' \rangle_{L^2_{ML}} + p(\mu_F)\phi(\mu_F) - S_0 E(t)\phi(0) = \langle [\beta(\mu) - \alpha]\, p, \phi \rangle_{L^2_{ML}}\,.$$

Repeating the above process for the equation for $m(t, \nu)$, we obtain the following weak formulation of the problem which should hold for all $\phi \in H^1_{ML}$, $\psi \in H^1_{AL}$:

$$\langle \dot{p}, \phi \rangle_{L^2_{ML}} - \langle p, \phi' \rangle_{L^2_{ML}} + p(\mu_F)\phi(\mu_F) - S_0 E(t)\phi(0) = \langle [\beta(\mu) - \alpha]\, p, \phi \rangle_{L^2_{ML}} \quad (44)$$

$$\langle \dot{m}, \psi \rangle_{L^2_{AL}} - \langle m, \psi' \rangle_{L^2_{AL}} + m(\nu_F)\psi(\nu_F) - p(\mu_F)\psi(0) = \langle -\gamma m, \psi \rangle_{L^2_{AL}} \quad (45)$$

$$\dot{E} + k_E E = f(m)(t). \quad (46)$$

7 Finite Element Formulation

We employ the method of finite elements, which is a general technique to construct an approximate solution to a boundary value problem [1], to rewrite the equation as a system of ordinary differential equations.

7.1 Basis Elements

Let $0 = \mu_1 < \mu_2 < \ldots < \mu_N = \mu_F$ be a uniform partition of the interval $[0, \mu_F]$ into $N - 1$ finite subintervals of length $h = \frac{\mu_F}{N-1}$.

We take as basis elements the piecewise linear continuous functions, ϕ_j, $j = 1, \ldots, N$, given by

$$\phi_j(\mu) = \begin{cases} \frac{\mu - \mu_{j-1}}{h}, & \mu_{j-1} \le \mu \le \mu_j, \\ \frac{\mu_{j+1} - \mu}{h}, & \mu_j \le \mu \le \mu_{j+1}, \\ 0 & 0 \le \mu \le \mu_{j-1} \text{ or } \mu_{j+1} \le \mu \le \mu_F, \end{cases}$$

with derivatives

$$\phi_j'(\mu) = \begin{cases} \frac{1}{h}, & \mu_{j-1} < \mu < \mu_j, \\ \frac{-1}{h}, & \mu_j < \mu < \mu_{j+1}, \\ 0 & 0 < \mu < \mu_{j-1} \text{ or } \mu_{j+1} < \mu < \mu_F. \end{cases}$$

Note that each $\phi_j \in H^1_{ML}$.

Similarly, we let $0 = \nu_1 < \nu_2 < \ldots < \nu_R = \nu_F$ be a uniform partition of the interval $[0, \nu_F]$ into $R - 1$ finite subintervals of length $h = \frac{\nu_F}{R-1}$. Again, we use piecewise linear continuous functions, $\psi_k \in H^1_{AL}$, where $k = 1, \ldots, R$, and ψ_k is defined in a manner similar to that of ϕ_j above but on the interval $[0, \nu_F]$.

7.2 Finite Element Approximation

We define the Galerkin finite element approximation $p(t,\mu) = \sum_{i=1}^{N} a_i(t)\phi_i(\mu)$, where ϕ_i is as defined in Section 7.1, and substitute it into equation (44) to obtain

$$\begin{aligned}\int_0^{\mu_F} \sum_{i=1}^{N} a_i'(t)\phi_i(\mu)\phi_j(\mu)d\mu + \sum_{i=1}^{N} a_i(t)\phi_i(\mu_F)\phi_j(\mu_F) & \\ -S_0E(t)\phi_j(0) - \int_0^{\mu_F} \sum_{i=1}^{N} a_i(t)\phi_i(\mu)\phi_j'(\mu)d\mu & \\ = \int_0^{\mu_D} \beta \sum_{i=1}^{N} a_i(t)\phi_i(\mu)\phi_j(\mu)d\mu - \int_0^{\mu_F} \alpha \sum_{i=1}^{N} a_i(t)\phi_i(\mu)\phi_j(\mu)d\mu, &\end{aligned}$$

where $j = 1, 2, \ldots, N$. We make simplifications to find

$$\begin{aligned}\sum_{i=1}^{N} a_i'(t) \int_0^{\mu_F} \phi_i(\mu)\phi_j(\mu)d\mu + \sum_{i=1}^{N} a_i(t)\phi_i(\mu_F)\phi_j(\mu_F) & \\ -S_0E(t)\phi_j(0) - \sum_{i=1}^{N} a_i(t) \int_0^{\mu_F} \phi_i(\mu)\phi_j'(\mu)d\mu & \\ = \sum_{i=1}^{N} a_i(t) \int_0^{\mu_D} \beta\phi_i(\mu)\phi_j d\mu - \sum_{i=1}^{N} a_i(t) \int_0^{\mu_F} \alpha\phi_i(\mu)\phi_j(\mu)d\mu & \\ \sum_{i=1}^{N} a_i'(t) \int_0^{\mu_F} \phi_i(\mu)\phi_j(\mu)d\mu + \sum_{i=1}^{N} a_i(t)\phi_i(\mu_F)\phi_j(\mu_F) & \\ -S_0E(t)\phi_j(0) - \sum_{i=1}^{N} a_i(t) \int_0^{\mu_F} \phi_i(\mu)\phi_j'(\mu)d\mu & \\ = \sum_{i=1}^{N} a_i(t) \left\{ \int_0^{\mu_D} \beta\phi_i(\mu)\phi_j(\mu)d\mu - \int_0^{\mu_F} \alpha\phi_i(\mu)\phi_j(\mu)d\mu \right\} & \\ \sum_{i=1}^{N} a_i'(t) \int_0^{\mu_F} \phi_i(\mu)\phi_j(\mu)d\mu + \sum_{i=1}^{N} a_i(t) \left\{ \phi_i(\mu_F)\phi_j(\mu_F) - \int_0^{\mu_F} \phi_i(\mu)\phi_j'(\mu)d\mu \right. & \\ \left. -\beta \int_0^{\mu_D} \phi_i(\mu)\phi_j(\mu)d\mu + \alpha \int_0^{\mu_F} \phi_i(\mu)\phi_j(\mu)d\mu \right\} & \\ = S_0E(t)\phi_j(0) &\end{aligned}$$

Thus, we have approximated the partial differential equation for $p(t,\mu)$ by an N-dimensional system of ordinary differential equations for the coefficients $a_i(t)$.

Let $m(t,\nu) = \sum_{k=1}^{R} b_k(t)\psi_k(\nu)$, and upon substitution into equation 45, we obtain

$$\begin{aligned}\int_0^{\nu_F} \sum_{k=1}^{R} b_k'(t)\psi_k(\nu)\psi_q(\nu)d\nu + \sum_{k=1}^{R} b_k(t)\psi_k(\nu_F)\psi_q(\nu_F) + \psi_q(0) \sum_{i=1}^{N} a_i(t)\phi_i(\mu_F) & \\ - \int_0^{\nu_F} \sum_{k=1}^{R} b_k(t)\psi_k(\nu)\psi_q'(\nu)d\nu &\end{aligned}$$

$$= -\int_0^{\nu_F} \gamma \sum_{k=1}^{R} b_k(t)\psi_k(\nu)\psi_q(\nu)d\nu,$$

which simplifies to

$$\sum_{k=1}^{R} b_k'(t)\int_0^{\nu_F} \psi_k(\nu)\psi_q(\nu)d\nu + \sum_{k=1}^{R} b_k(t)\psi_k(\nu_F)\psi_q(\nu_F) + \psi_q(0)\sum_{i=1}^{N} a_i(t)\phi_i(\mu_F)$$
$$- \sum_{k=1}^{R} b_k(t)\int_0^{\nu_F} \psi_k(\nu)\psi_q'(\nu)d\nu$$
$$= -\sum_{k=1}^{R} b_k(t)\int_0^{\nu_F} \gamma\psi_k(\nu)\psi_q(\nu)d\nu.$$

Collecting common terms we arrive at:

$$\sum_{k=1}^{R} b_k'(t)\int_0^{\nu_F} \psi_k(\nu)\psi_q(\nu)d\nu - \sum_{i=1}^{N} a_i(t)\phi_i(\mu_F)\psi_q(0)$$
$$+ \sum_{k=1}^{R} b_k(t)\left\{\psi_k(\nu_F)\psi_q(\nu_F) - \int_0^{\nu_F} \psi_k(\nu)\psi_q'(\nu)d\nu + \gamma\int_0^{\nu_F} \psi_k(\nu)\psi_q(\nu)d\nu\right\}$$
$$= 0$$

Thus, the system given by equations (8) - (15) can be approximated by the following system of $N + R + 1$ ordinary differential equations.

$$\sum_{i=1}^{N} a_i'(t)\int_0^{\mu_F} \phi_i(\mu)\phi_j(\mu)d\mu$$
$$+ \sum_{i=1}^{N} a_i(t)\left\{\phi_i(\mu_F)\phi_j(\mu_F) - \int_0^{\mu_F} \phi_i(\mu)\phi_j'(\mu)d\mu\right.$$
$$\left. -\beta\int_0^{\mu_D} \phi_i(\mu)\phi_j(\mu)d\mu + \alpha\int_0^{\mu_F} \phi_i(\mu)\phi_j(\mu)d\mu\right\}$$
$$= S_0E(t)\phi_j(0) \qquad j = 1, 2, \ldots, N \tag{47}$$
$$\sum_{k=1}^{R} b_k'(t)\int_0^{\nu_F} \psi_k(\nu)\psi_q(\nu)d\nu - \sum_{i=1}^{N} a_i(t)\phi_i(\mu_F)\psi_q(0)$$
$$+ \sum_{k=1}^{R} b_k(t)\left\{\psi_k(\nu_F)\psi_q(\nu_F) - \int_0^{\nu_F} \psi_k(\nu)\psi_q'(\nu)d\nu + \gamma\int_0^{\nu_F} \psi_k(\nu)\psi_q(\nu)d\nu\right\}$$
$$= 0 \qquad q = 1, 2, \ldots, R \tag{48}$$
$$\frac{dE(t)}{dt} + k_E E(t) = f\left(\sum_{k=1}^{R} b_k\psi_k\right)(t) \tag{49}$$

with initial conditions

$$\sum_{i=1}^{N} a_i(0)\phi_i(\mu) = p_0(\mu) \tag{50}$$

$$\sum_{k=1}^{R} b_k(0)\psi_k(\nu) = m_0(\nu) \tag{51}$$

$$E(0) = E_0. \tag{52}$$

Equations (47) - (49) can be rewritten in the matrix form

$$\tilde{M}\dot{\vec{x}}(t) + \tilde{A}\vec{x}(t) = \vec{g}(\vec{b})(t) \tag{53}$$

where

$$\vec{x} = \begin{bmatrix} \vec{a} \\ \vec{b} \\ E \end{bmatrix}$$

and

$$\vec{g} = \begin{bmatrix} \vec{0} \\ \vec{0} \\ f(\vec{b})(t) \end{bmatrix}.$$

8 Numerical Simulations

For the numerical simulations of equation (53), we took ϕ and ψ to be linear splines defined on uniform partitions of $0 \leq \mu \leq \mu_F$ and $0 \leq \nu \leq \nu_F$ respectively. We chose $N = 250$ and $R = 125$. We note that the reason we used more elements for p was because the terminal boundary at $\mu = \mu_F$ of $p(t, \mu)$ was used as the initial boundary condition at $\nu = 0$ for $m(t, \nu)$. Because of the form of this system, as is evident by the notation in equation (53), we used the differential algebraic equation solver in MATLAB instead of inverting the matrix.

Although we would eventually like to use the concentrations for phenol and hydroquinone in the richly perfused tissue as input into the death rate term α, here we will first show results based on initial depletion of precursor cells or depletion of precursor and mature cells.

We take the normal levels of mature cells to be 3.5, which has units of 10^{11} erythrocytes per kilogram body weight. The normal precursor population is equal to 1% of the mature cell population since progenitor cells, which are the major component of the precursor cells, comprise 1% of the hematopoietic population [2, 23]. For the precursor cells, we assume the initial condition $p_0(\mu)$ is linear for

Table 1: Parameter Values for the Erythropoiesis Model using the Hill Feedback Function

Parameter	Value
μ_D	3
μ_F	5.9
ν_F	50
S_0	4.45×10^{-7}
k_E	6.65
β	2.773
α	0
γ	0.01
a	15600
K	0.0382
r	6.96

$0 \leq \mu < \mu_D$ and constant for $\mu \in [\mu_D, \mu_F]$. For the mature cells, the initial condition $m_0(\nu)$ is constant. For a human, the normal concentration of Epo is believed to be between 10 and 25 mU/mL plasma, although values in the range of 3 to 18,000 mU/mL plasma have been reported [2]. We take our initial condition, or the normal state, to be 15 mU/mL plasma.

We chose the other parameters in a similar fashion to those of Bélair, Mahaffy, and Mackey [2, 3, 17, 18, 19]. The values of the parameters that were used are shown in Table 1. We chose $\mu_D = 3$, as the period of progenitor cell maturation is approximately 3 days [2]. We took μ_F, the final maturity level of precursor cells, to be 5.9 days and ν_F, the final age of mature cells, to be 50 days [3, 18]. Although different values of β, the rate of birth of precursor cells while they are still dividing, have been used previously, we chose β to be 2.773 days^{-1} [3]. The death rate of mature cells γ is thought to be in the range of 0.001 to 0.1 days^{-1} [2, 3, 17]; we took γ=0.01, which is certainly in that range. The half-life of Epo has been reported be be as short as 2.5 hours and as long as 1 to 2 days [2, 18, 30]. We chose the half-life of 2.5 hours, which corresponds to $k_E = 6.65$ days^{-1}, similar to that used in several previous studies [2, 3, 18]. The values used previously for S_0 have ranged from

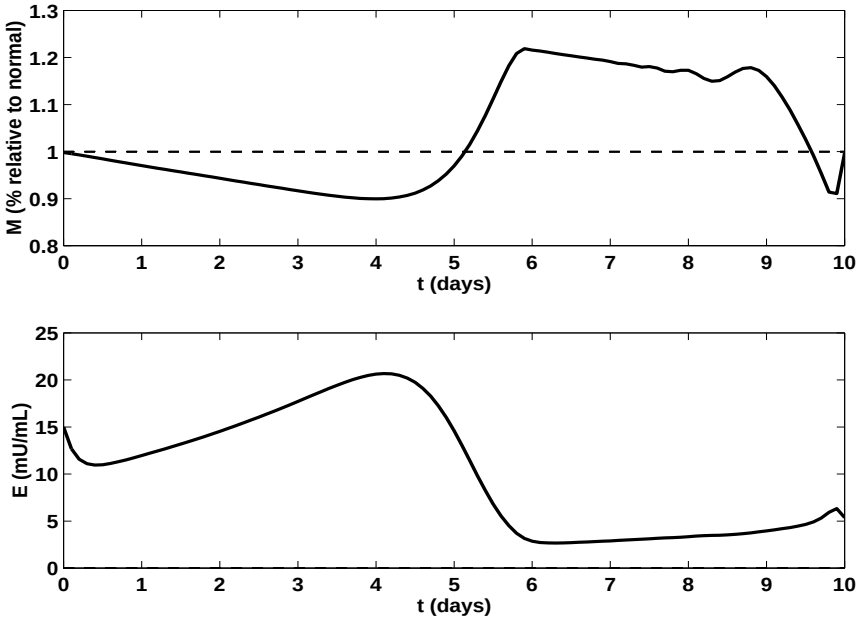

Figure 5: Mature cell and erythropoietin response following precursor cell depletion using Hill function feedback

4.45×10^{-7} ($\times 10^{11}$ erythrocytes/kg body weight $\times$ mL plasma/mU Epo/day) [17, 19] to 0.00372 [18]; we choose $S_0 = 4.45 \times 10^{-7}$. We use the following values in the Hill function: $a = 15,600$, $K = 0.0382$, and $r = 6.96$ [2, 17].

For this study, we began by looking at two simulations: the first in which precursor cells were depleted by 5%, that is, 95% of normal, but the mature cells were not depleted and the second in which precursor and mature cells were initially at only 95% of normal. One could think of this physically as the body having been exposed to a toxic substance, such as benzene, the cells being depleted, and then the model examining the body's response. These results are shown in Figures 5 and 6 respectively. In each set of plots, the top plot shows $M(t)$ whereas the lower plot is $E(t)$. The inverse relation between $M(t)$ and $E(t)$ is obvious from these plots; Epo increases when the total number of mature cells is less than the normal level and decreases when the number of mature cells is greater than the normal level needed by the body. We see that the rise in Epo overshoots and causes an overproduction of mature cells. We note that the depletion of precursor and mature cells causes the concentration of Epo to rise more than in the case where just the precursor cells were depleted.

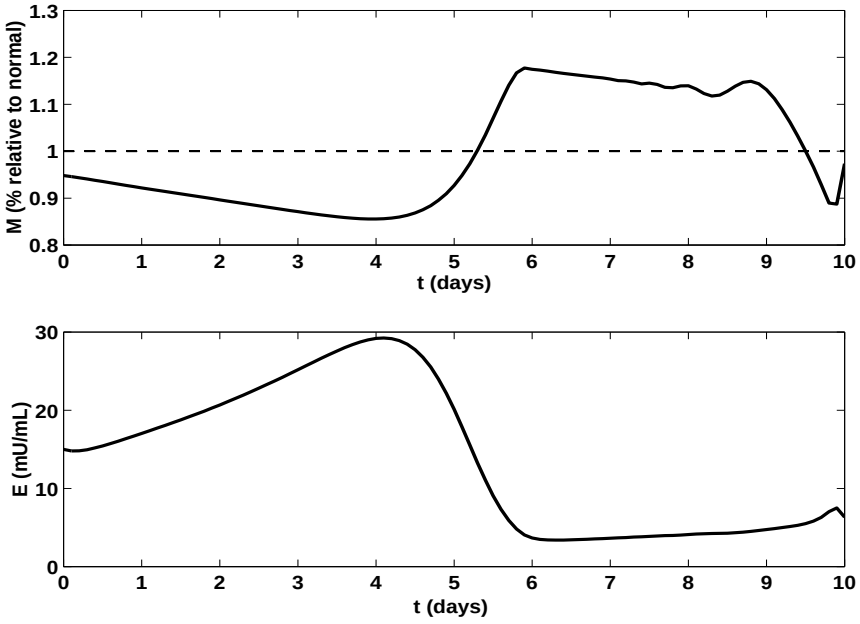

Figure 6: Mature cell and erythropoietin response following precursor and mature cell depletion using Hill function feedback

9 Optimal Control

9.1 Problem Formulation

In previous studies and in the first part of this study, the feedback mechanism has been represented by the Hill function. However, it was not able to maintain the normal level of mature cells. Next we will formulate an optimal control problem to find an optimal feedback function such that we can track the reference signal, which is $M(t)$ in this problem. That is, we want to find a feedback function in which we regulate and maintain the normal number of red blood cells in the body, which is the type of regulation the renal sensors are effecting to cause the release of Epo.

We first write our approximate simulation system in the form:

$$\begin{aligned} \tilde{M}\dot{\vec{x}}(t) &= -\tilde{A}\vec{x}(t) + \vec{g}(\vec{b})(t) \\ \vec{x}(0) &= \vec{x}_0 \end{aligned}$$

where

$$\vec{x}(t) = \begin{bmatrix} \vec{a} \\ \vec{b} \\ E \end{bmatrix}$$

and

$$\vec{g}(\vec{b})(t) = \begin{bmatrix} \vec{0} \\ \vec{0} \\ f(\vec{b})(t) \end{bmatrix}$$

where $f(\vec{b})(t)$ is the Hill function which has been used previously. We now rewrite the differential equation as

$$\dot{\vec{x}}(t) = -\tilde{M}^{-1}\tilde{A}\vec{x}(t) + \tilde{M}^{-1}\begin{bmatrix} 0 \\ 0 \\ B_u \end{bmatrix} u(t)$$

in order to formulate an optimal tracking problem of finding a feedback control $u(t)$ so as to maintain the normal level of mature red blood cells in the body. Now, let $A = -\tilde{M}^{-1}\tilde{A}$ and $B = \tilde{M}^{-1}[\vec{0}\ \ \vec{0}\ \ B_u]^T$, where B_u is a positive constant. Then we can write the system as

$$\dot{\vec{x}}(t) = A\vec{x}(t) + Bu(t) \tag{54}$$

$$\vec{x}(0) = \vec{x}_0 \tag{55}$$

where $u(t)$ is our control function, thus replacing the nonlinear function $\vec{g}$ by a linear function u.

Let $z(t)$ denote the tracking variable, which is given by

$$\begin{aligned} z(t) &= M(t) \\ &= \int_0^{\nu_F} m(t,\nu)d\nu \\ &\approx \frac{dR}{2}m(t,\nu_1) + dR\sum_{k=2}^{R-2} m(t,\nu_k) + \frac{3dR}{2}m(t,\nu_{R-1}) \\ &= H\vec{x}(t) \end{aligned}$$

where H is of the form

$$H = \left[\vec{0}\ \ \frac{dR}{2}\ \ dR\ \ dR\ \ \cdots\ \ dR\ \ \frac{3dR}{2}\ \ 0\ \ 0\right].$$

For the erythropoiesis model, we want $z(t)$ to track a reference signal $r_M = 3.5$, which is the normal value of $M(t)$. That is, r_M is the normal number times 10^{11} per kilogram body weight of mature red blood cells in the body.

The optimal tracking problem is to find a feedback function $u(t)$ to minimize the performance measure

$$\begin{aligned} J(u) &= \frac{1}{2}\int_0^\infty \Big\{ \Big[z(t) - r_M\Big] q_d \Big[z(t) - r_M\Big] + u(t) r_d u(t) \Big\} dt \\ &= \frac{1}{2}\int_0^\infty \Big\{ \Big[H\vec{x}(t) - r_M\Big] q_d \Big[H\vec{x}(t) - r_M\Big] + u(t) r_d u(t) \Big\} dt \\ &= \frac{1}{2}\int_0^\infty \Big\{ q_d \Big[H\vec{x}(t) - r_M\Big]^2 + r_d u^2(t) \Big\} dt, \end{aligned}$$

where q_d and r_d are positive design parameters, subject to

$$\begin{aligned} \dot{\vec{x}}(t) &= A\vec{x}(t) + Bu(t) \\ z(t) &= H\vec{x}(t) \\ \vec{x}(0) &= \vec{x}_0. \end{aligned}$$

9.2 Necessary Conditions

We define the Hamiltonian:

$$\mathcal{H}(\vec{x}(t), u(t), \vec{y}(t)) = \frac{1}{2} q_d \Big[H\vec{x}(t) - r_M\Big]^2 + \frac{1}{2} r_d u^2(t) + \vec{y}^T(t)\Big[A\vec{x}(t) + Bu(t)\Big].$$

Then the necessary conditions for optimality are given by [13, 15]:

$$\begin{aligned} \dot{\vec{x}}^*(t) &= \frac{\partial \mathcal{H}}{\partial \vec{y}} \\ &= A\vec{x}^*(t) + Bu^*(t) \qquad (56) \\ \dot{\vec{y}}^*(t) &= -\frac{\partial \mathcal{H}}{\partial \vec{x}} \\ &= -q_d H^T \Big[H\vec{x}^*(t) - r_M\Big] - A^T \vec{y}^*(t) \qquad (57) \\ 0 &= \frac{\partial \mathcal{H}}{\partial u} \\ &= r_d u^*(t) + B^T \vec{y}^*(t). \qquad (58) \end{aligned}$$

From equation (58), we find that

$$u^*(t) = -\frac{1}{r_d} B^T \vec{y}^*(t). \qquad (59)$$

Now we assume that

$$\vec{y}^*(t) = \Pi\vec{x}^*(t) + \vec{s}. \tag{60}$$

Taking the derivative of equation (60) and substituting into equation (57), we obtain the following relation:

$$\Pi\dot{\vec{x}}^*(t) = -q_d H^T\Big[H\vec{x}^*(t) - r_M\Big] - A^T\vec{y}^*(t).$$

We now do a series of substitutions, first substituting equation (56) for $\dot{\vec{x}}^*(t)$

$$\Pi\Big[A\vec{x}^*(t) + Bu^*(t)\Big] = -q_d H^T\Big[H\vec{x}^*(t) - r_M\Big] - A^T\vec{y}^*(t),$$

then equation (59) for $u^*(t)$

$$\Pi\left[A\vec{x}^*(t) - B\frac{1}{r_d}B^T\vec{y}^*(t)\right] = -q_d H^T\Big[H\vec{x}^*(t) - r_M\Big] - A^T\vec{y}^*(t),$$

and finally equation (60) for $\vec{y}^*(t)$

$$\Pi\left\{A\vec{x}^*(t) - B\frac{1}{r_d}B^T\Pi\Big[\vec{x}^*(t) + \vec{s}\Big]\right\} = -q_d H^T\Big[H\vec{x}^*(t) - r_M\Big] - A^T\Big[\Pi\vec{x}^*(t) + \vec{s}\Big].$$

Rearranging the terms we have

$$\left[\Pi A + A^T\Pi - \frac{1}{r_d}BB^T\Pi + q_d H^T H\right]\vec{x}^*(t) + \left[-\frac{1}{r_d}\Pi BB^T\vec{s} - q_d r_M H^T + A^T\vec{s}\right] = 0.$$

Since we desire this to be true for all $\vec{x}^*(t)$, we require

$$\Pi A + A^T\Pi - \frac{1}{r_d}BB^T\Pi + q_d H^T H = 0 \tag{61}$$

which is the algebraic Ricatti equation, and

$$\vec{s} = q_d r_M\left(A^T - \frac{1}{r_d}\Pi BB^T\right)^{-1}H^T, \tag{62}$$

which is sometimes called the tracking equation.

We now return to our assumed form of $\vec{y}^*(t)$ and using equation (62), we find

$$\begin{aligned}\vec{y}^*(t) &= \Pi\vec{x}^*(t) + \vec{s} \\ &= \Pi\vec{x}^*(t) + q_d r_M\left(A^T - \frac{1}{r_d}\Pi BB^T\right)^{-1}H^T.\end{aligned}$$

Thus, the optimal feedback control $u^*(t)$ is given by

$$\begin{aligned}u^*(t) &= -\frac{1}{r_d}B^T\vec{y}^*(t) \\ &= -\frac{1}{r_d}B^T\Pi\vec{x}^*(t) - \frac{1}{r_d}B^T q_d r_M\left(A^T - \frac{1}{r_d}\Pi BB^T\right)^{-1}H^T.\end{aligned} \tag{63}$$

Table 2: Set 1 of Parameter Values for the Erythropoiesis Model using the Optimal Feedback Function

Parameter	Value
μ_D	3
μ_F	5.9
ν_F	50
S_0	0.00008
k_E	6.65
β	1.5
α	0
γ	0.001
q_d	100
r_d	10^{-4}
B_u	1.5

9.3 Numerical Results

In this section, numerical simulations were carried out to synthesize the feedback given by equation (63). For these computations, we took $N = 25$ and $R = 75$. These values of N and R were used in order to provide a better approximation of $m(t, \nu)$ since m is used in the tracking term. The parameter values that were used in this case can be found in Table 2; although these values differ from those used with the Hill function simulations (see Table 1), they are still all within reasonable physiological ranges of values. We again began with a 5% depletion of precursor cells or precursor and mature cells. These results in which the feedback was of the form of the optimal control given in equation (63) are presented in Figures 7 and 8. As depicted in Figure 8, it also took a longer period of time to return the system to normal levels of M than when the Hill function was used, although the Hill function did not maintain this normal value, only passed through it. We note though that the optimal control brought the total number of mature cells M back closer to the normal value much more gradually than when the Hill function was used and there

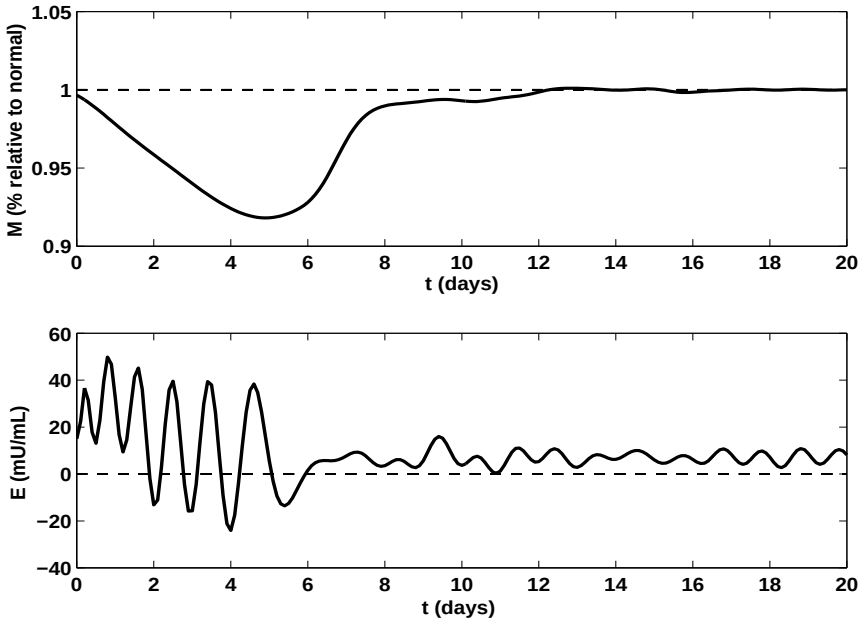

Figure 7: Mature cell and erythropoietin response following precursor cell depletion using optimal feedback with parameters from Table 2

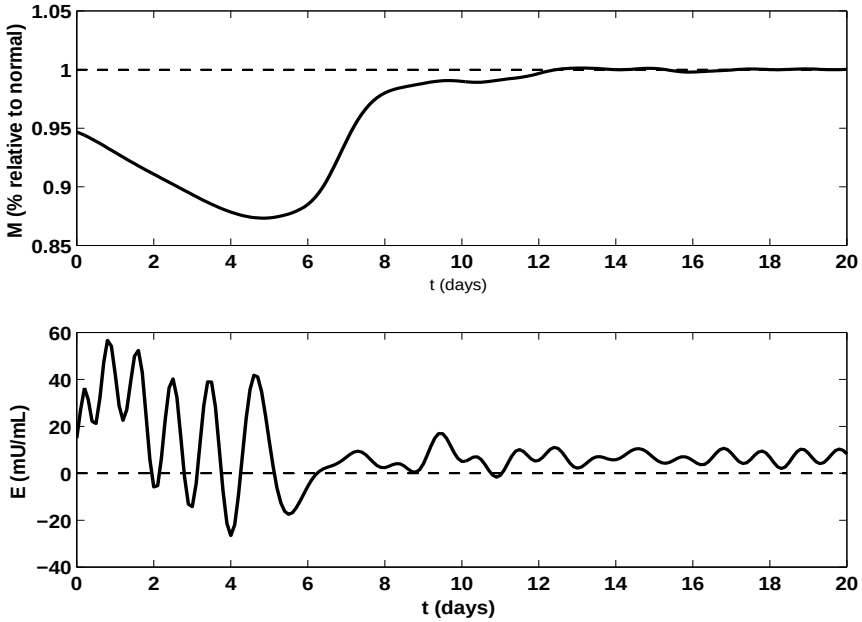

Figure 8: Mature cell and erythropoietin response following precursor cell and mature cell depletion using optimal feedback with parameters from Table 2

Table 3: Set 2 of Parameter Values for the Erythropoiesis Model using the Optimal Feedback Function

Parameter	Value
μ_D	3
μ_F	5.9
ν_F	50
S_0	0.00008
k_E	66.5
β	1.1
α	0
γ	0.01
q_d	9500
r_d	8×10^{-6}
B_u	1.5

was less overproduction of cells. The maximum values of the Epo concentration are within a normal range, but the concentrations that produced optimal tracking also acquired negative values, which we know are not physically possible.

We again assumed an initial depletion of 5% of precursor cells and then precursor and mature cells. We then used the set of parameters given in Table 3. We note that the value of k_E is not physiologically realistic. These simulation results are shown in Figures 9 and 10. Here, the system did return to normal level of M much more quickly than when the parameter values in Table 2 were used. There was more fluctuation in the concentration of Epo, but less of this fluctuation was in the negative range. Thus, although the parameter values may not all be physiologically realistic, they did produce a more physically plausible outcome.

9.4 Suboptimal Control

We note that, from Figure 11, E was negative when the feedback control, $u(t)$, had negative values. One approach (commonly used in engineering applications) that we

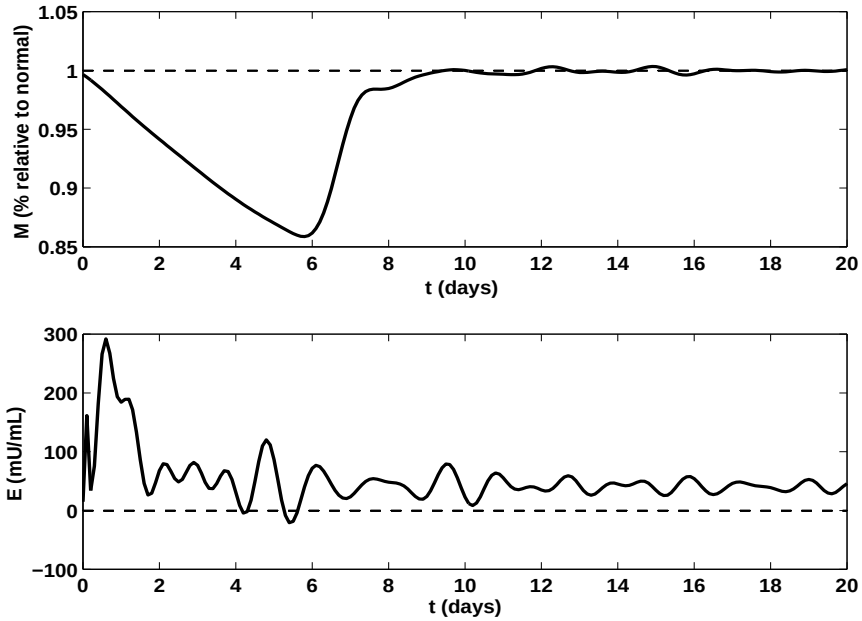

Figure 9: Mature cell and erythropoietin response following precursor cell depletion using optimal feedback with parameters from Table 3

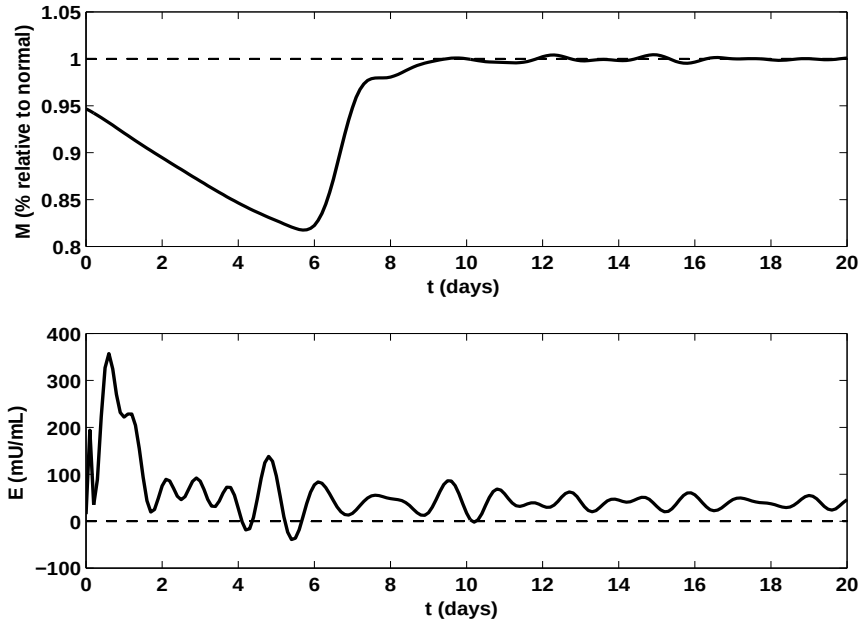

Figure 10: Mature cell and erythropoietin response following precursor and mature cell depletion using optimal feedback with parameters from Table 3

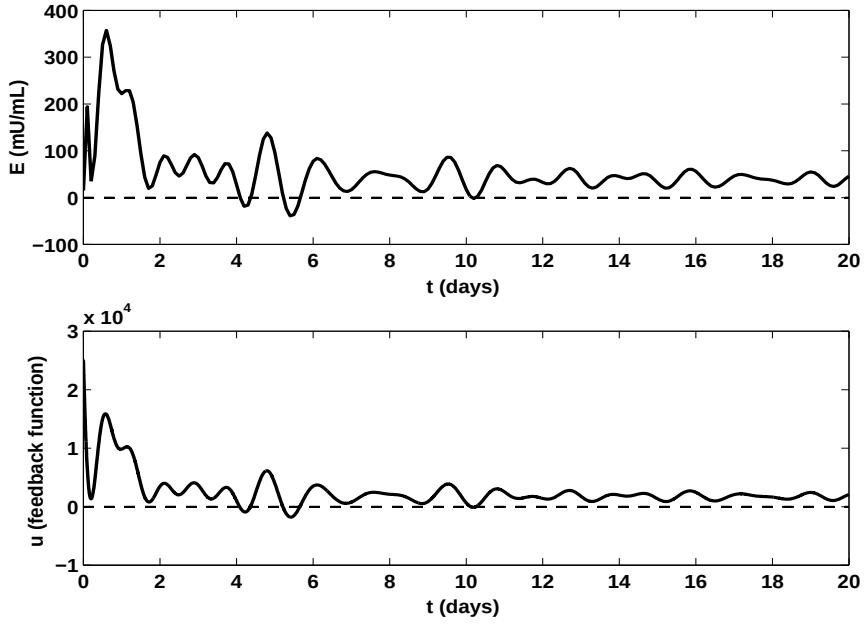

Figure 11: Erythropoietin response and feedback function following precursor cell and mature cell depletion using optimal feedback with parameters from Table 3

considered was to reset $u(t)$ to be zero whenever its value became negative. This results in a suboptimal control. However, as depicted in Figures 12 and 13, using the suboptimal control, the mature cell level is tracked well, maintaining a normal level of cells, and at the same time the level of the hormone Epo is now nonnegative.

We then considered the situation where we began in a normal state but had a cell death rate of 5% for precursor as well as mature cells; in other words, $\alpha = 0.05$ and $\gamma = 0.05$. This would be equivalent to a constant level of benzene toxicity in the bone marrow killing off precursor cells and mature cells in the blood dying off at a slightly higher rate (0.05 instead of 0.01) than was previously used. All other values were taken to be the same as in Table 3. These results are shown in Figure 14. Despite the fact that precursor and mature cells were constantly dying off, the suboptimal control did a good job tracking the normal level of total mature cells M in the body.

We note that the concentrations of Epo found using the optimal and suboptimal control model were higher and fluctuate more than when the Hill function was used to represent the feedback mechanism. But, a wide range of Epo values from 3 to 18,000 has been observed, so that the range seen in our numerical simulations is realistic [2]. It is also noted that although Epo levels vary more than with the Hill

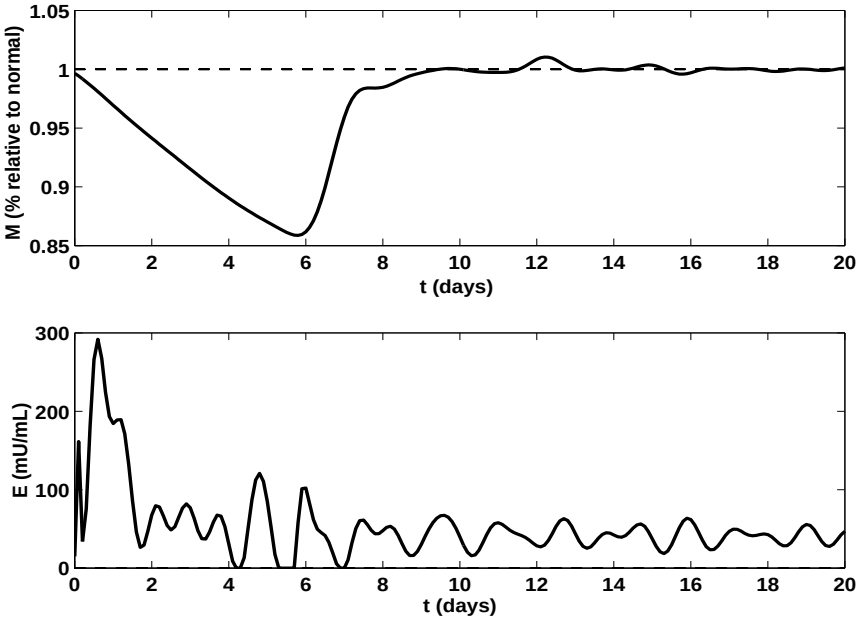

Figure 12: Mature cell and erythropoietin response following precursor cell depletion using suboptimal feedback with parameters from Table 3

function, there was much less fluctuation in the number of mature cells in the body and the normal level of mature cells was maintained when the optimal or suboptimal form of the feedback function was used.

10 Discussion

In this study we have examined an age-structured model for erythropoiesis. By using the method of characteristics with a modified version of the method of steps, we eliminate the need for the age-structured population equations for p and m and replace them with a delay differential equation for the total mature population $M(t)$. This results in a new system of delay differential equations for $M(t)$ and $E(t)$. Standard existence and uniqueness results for delay differential equations were then used to guarantee the existence and uniqueness of the solution to the model. The system was then written in weak form and a numerical approximation to the solution of the system was found using finite elements. It should be noted that in previous studies the system had been simplified to a system of delay differential equations; thus, to our knowledge, this is the first time the system of coupled partial and

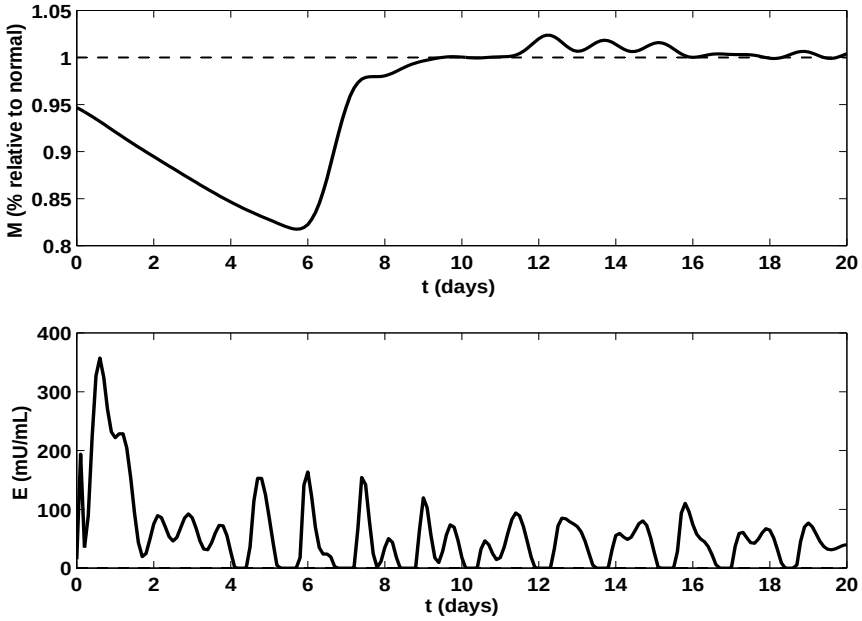

Figure 13: Mature cell and erythropoietin response following precursor and mature cell depletion using suboptimal feedback with parameters from Table 3

ordinary differential equations has been solved numerically. Finally, we used optimal control theory to track the total number of mature cells and to find an optimal form of the feedback function of Epo, which determines the number of proliferating precursor cells that are recruited from the stem cell population. In earlier studies, a Hill function, which is a standard function often used to characterize unknown enzyme kinetics, had been used to represent this nonlinear feedback. The results in the literature using the Hill function establish that this function is not a very good representation of the feedback, as evidenced by the fact that the Epo released using this function results in underproduction or overproduction of cells and does not maintain normal levels. Suboptimal linear controls were then obtained in order to keep the concentration of Epo in the nonnegative range. We note that both the optimal and suboptimal linear controls did an excellent job in tracking the total number of mature cells. Computations were done for various biological scenarios.

Although there were gains made through this research in solving the erythropoiesis model as system of partial and ordinary differential equations, there were multiple simplifications that were made. In the future, we hope to look at a velocity of maturation for the precursor cells that is dependent upon the Epo level

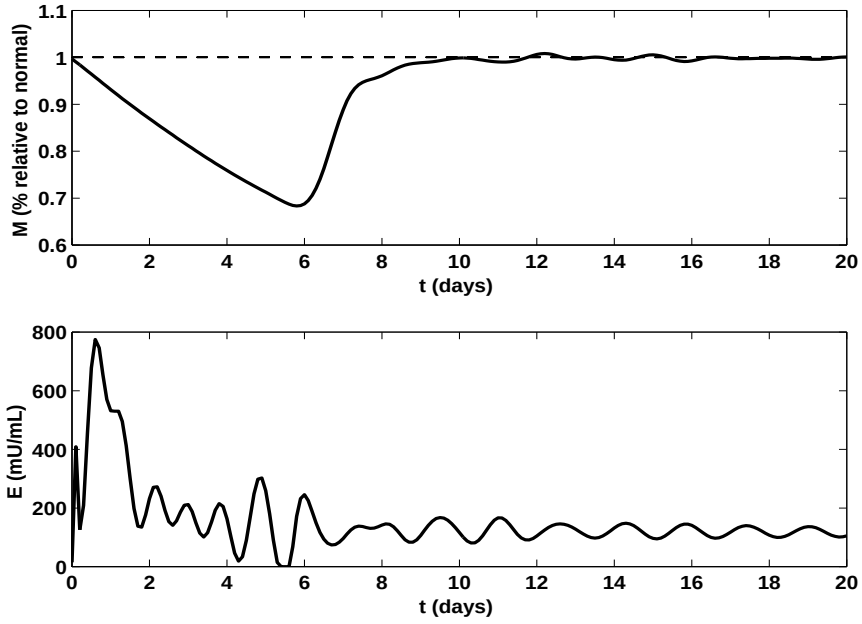

Figure 14: Mature cell and erythropoietin response with continuous death of precursor and mature cells using suboptimal feedback

rather than being constant as well as cell death for mature cells that is a function of the cell age ν. Additionally, we would like to formulate β as a function of both μ and E. This would create new issues in both the theoretical and numerical aspects of solving the model since the partial differential equation for $p(t, \mu)$ would involve nonlinearity in terms of multiple state variables. This would create new complexities in the control and tracking problem as well. Also, some work by Mahaffy et al. [18] suggests that the final age of mature cells should not be fixed but be a function of time, which would present additional new challenges.

In the future we hope to use the results of the PBPK model as direct time-course input into the precursor death rate term of the erythropoiesis model. We would also like to extend the model to include other lineages of hematopoiesis, such as granulopoiesis and thrombopoiesis. The model could also be modified in such a way to include mutations in blood cells and consider "parallel" age-structured models representing the maturation of the different lineages of mutated cells. This could lead to a model in which the possibility of tumors following benzene exposure could be predicted.

Acknowledgments

Cammey E. Cole was supported via a fellowship from the CIIT Centers for Health Research while she was a graduate student in the Center for Research in Scientific Computation at North Carolina State University.

Appendix: Model Symbols

t	Time (days)
μ	Maturity level of precursor cells (days)
ν	Age of mature cells (days)
$p(t, \mu)$	Number of precursor cells at time t and maturity μ
$m(t, \nu)$	Number of mature cells at time t and age ν
$E(t)$	Concentration of erythropoietin at time t (mU/mL plasma)
μ_D	Maturity level at which precursor cells stop dividing (days)
μ_F	Oldest maturity level of precursor cells (days)
ν_F	Oldest age of mature cells (days)
$M(t)$	Total number of mature cells at time t ($\times 10^{11}$ erythrocytes/kg body weight)
S_0	Rate of cell recruitment of cells into the proliferating precursor population ($\times 10^{11}$ erythrocytes/kg body weight $\times$ mL plasma/mU Epo/day)
β	Birth rate of precursor cells (days^{-1})
α	Death rate of precursor cells (days^{-1})
γ	Death rate of mature cells (days^{-1})
k_E	Decay rate of Erythropoietin (days^{-1})
$V(E)$	Velocity of maturation of precursor cells
W	Rate of aging of mature cells
a, K, r	Parameters in the Hill function

References

[1] Eric B. Becker, Graham F. Carey, and J. Tinsley Oden. *Finite Elements: An Introduction, Volume 1.* Prentise-Hall, 1981.

[2] Jacques Bélair, Michael C. Mackey, and Joseph M. Mahaffy. Age-structured and two-delay models for erythropoiesis. *Mathematical Biosciences*, 128:317–346, 1995.

[3] Jacques Bélair and Joseph M. Mahaffy. Variable maturation velocity and parameter sensitivity in a model for haematopoiesis. *IMA Journal of Mathematics Applied in Medicine and Biology*, 18:193–211, 2001.

[4] William E. Boyce and Richard C. DiPrima. *Elementary Differential Equations and Boundary Value Problems.* Wiley and Sons, 6th edition, 1997.

[5] Cammey E. Cole, Paul M. Schlosser, and Hien T. Tran. A multicompartment liver-based pharmacokinetic model for benzene and its metabolites in mice. *J. of Mathematical Biology*, submitted.

[6] Cammey E. Cole, Hien T. Tran, and Paul M. Schlosser. Physiologically based pharmacokinetic modeling of benzene metabolism in mice through extrapolation from in vitro to in vivo. *J. Toxicol. Environ. Health*, pages 439–465, 2001.

[7] R. D. Driver. *Ordinary and Delay Differential Equations.* Springer-Verlag, 1977.

[8] Rodney D. Driver. *Introduction to Ordinary Differential Equations.* Harper and Row, 1978.

[9] David W. Golde, Martin J. Cline, Donald Metcalf, and C. Fred Fox. *Hematopoietic Cell Differentiation.* Academic Press, 1978.

[10] John W. Harris and Robert W. Kellermeyer. *The Red Cell Production, Metabolism, and Destruction: Normal and Abnormal.* Harvard University Press, 1963.

[11] George Kalf. Recent advances in the metabolism and toxicity of benzene. *CRC Crit. Rev. Toxicol.*, 18:141–159, 1987.

[12] James Keener and James Sneyd. *Mathematical Physiology.* Springer, 1998.

[13] Donald E. Kirk. *Optimal Control: An Introduction.* Prentice-Hall, 1970.

[14] Agnes Legathe, Betty-Ann Hoener, and Thomas N. Tozer. Pharmacokinetic interaction between benzene metabolites, phenol and hydroquinone, in B6C3F1 mice. *Toxicol. Appl. Pharmacol.*, 124:131–138, 1994.

[15] Frank L. Lewis and Vassilis L. Syrmos. *Optimal Control*. John Wiley & Sons, second edition, 1995.

[16] Laureen MacEachern, Robert Snyder, and Dabra Laskin. Alterations in the morphology and functional activity of bone marrow phagocytes following benzene treatment in mice. *Toxicol. Appl. Pharmacol.*, 117:147–154, 1992.

[17] Joseph M. Mahaffy. Age-structured modeling of hematopoiesis. *IMA Research Publication*, submitted, 1999.

[18] Joseph M. Mahaffy, Jacques C. Bélair, and Michael C. Mackey. Hematopoietic model with moving boundary condition and state dependent delay: Application in erythropoiesis. *J. Theor. Biol.*, 190:135–146, 1998.

[19] Joseph M. Mahaffy, Samuel W. Polk, and Roland K.W. Roeder. An age-structured model for erythropoiesis following a phlebotomy. Technical Report CRM-2598, Centre recherches mathématiques, Université de Montréal, 1999.

[20] Casare Maltoni, Barbara Conti, Guiliano Cotti, and Fiorella Belpoggi. Experimental studies on benzene carcinogenicity at the Bologna institute of oncology: Current results and ongoing research. *Am. J. Ind. Med.*, 7:415–446, 1985.

[21] Cesare Maltoni, Barbara Conti, and Giuliano Cotti. Benzene: a multipotential carcinogen. Results of long-term bioassays performed at the Bologna institute of oncology. *Am. J. Ind. Med.*, 4:589–630, 1983.

[22] A. Manitius. Optimal control for hereditary systems. In *Control Theory and Topics in Functional Analysis*, volume III. International Atomic Energy Agency, 1976.

[23] Donald Metcalf and Nicos Anthony Nicola. *The Hemopoietic Colony-Stimulating Factors: From biology to clinical applications*. Cambridge University Press, 1995.

[24] Dennis V. Parke. Personal reflections on 50 years of study in benzene toxicology. *Environ. Health Perspect.*, 104:1123–1128, December 1996.

[25] Lawrence Perko. *Differential Equations and Dynamical Systems.* Springer-Verlag, 2nd edition, 1996.

[26] Mark W. Powley and Gary P. Carlson. Species comparison of hepatic and pulmonary metabolism of benzene. *Toxicology*, 139:207–217, 1999.

[27] Stefan Scheding, Markus Loeffler, Stephan Schmitz, Hans-J. Siedel, and H.-Erich Wichmann. Hematoxic effects of benzene analyzed by mathematical modeling. *Toxicology*, 72:265–279, 1992.

[28] Martyn T. Smith. Overview of benzene-induced aplastic anaemia. *Eur. J. Haematol.*, 57:107–110, 1996.

[29] Lance Wallace. Major sources of exposure to benzene and other volatile organic chemicals. *Risk Anal.*, 10:59–64, 1990.

[30] William J. Williams, Ernest Beutler, Allan J. Erslev, and Marshall A. Lichtman. *Hematology.* McGraw-Hill, 4th edition, 1990.

[31] A. Yardley-Jones, D. Anderson, and D. V. Parke. The toxicity of benzene and its metabolism and molecular pathology in human risk assessment. *Br. J. Ind. Med.*, 48:437–444, 1991.